

THE EARLY BLAST WAVE OF THE 2010 EXPLOSION OF U SCORPII

J. J. DRAKE¹ AND S. ORLANDO²

¹ Harvard-Smithsonian Center for Astrophysics, 60 Garden Street, Cambridge, MA 02138, USA

² INAF–Osservatorio Astronomico di Palermo “G.S. Vaiana,” Piazza del Parlamento 1, 90134 Palermo, Italy
 Received 2010 February 25; accepted 2010 July 28; published 2010 August 20

ABSTRACT

Three-dimensional hydrodynamic simulations exploring the first 18 hr of the 2010 January 28 outburst of the recurrent nova U Scorpii have been performed. Special emphasis was placed on capturing the enormous range in spatial scales in the blast. The pre-explosion system conditions included the secondary star and a flared accretion disk. These conditions can have a profound influence on the evolving blast wave. The blast itself is shadowed by the secondary star, which itself gives rise to a low-temperature bow shock. The accretion disk is completely destroyed in the explosion. A model with a disk gas density of 10^{15} cm^{-3} produced a blast wave that is collimated and with clear bipolar structures, including a bipolar X-ray emitting shell. The degree of collimation depends on the initial mass of ejecta, energy of explosion, and circumstellar gas density distribution. It is most pronounced for a model with the lowest explosion energy (10^{43} erg) and mass of ejecta ($10^{-8} M_{\odot}$). The X-ray luminosities of three of six models computed are close to, but consistent with, an upper limit to the early blast X-ray emission obtained by the *Swift* satellite, the X-ray luminosity being larger for higher circumstellar gas density and higher ejecta mass. The latter consideration, together with estimates of the blast energy from previous outbursts, suggests that the mass of ejecta in the 2010 outburst was not larger than $10^{-7} M_{\odot}$.

Key words: methods: numerical – novae, cataclysmic variables – shock waves – stars: individual (U Sco) – X-rays: binaries

Online-only material: color figures

1. INTRODUCTION

U Scorpii was discovered to have entered its latest outburst on 2010 January 28 by amateur astronomer B. G. Harris (Schaefer et al. 2010). It is one of the best observed of the 10 recurrent novae known to date (e.g., Schaefer 2010), with a fairly constant recurrent cycle of 8–12 yr and a previous outburst in 1999. It comprises a white dwarf of mass $1.55 \pm 0.24 M_{\odot}$ and late-type star of mass $0.88 \pm 0.17 M_{\odot}$ in an orbit with a period of 1.23 days (Johnston & Kulkarni 1992; Thoroughgood et al. 2001; Schaefer 1990; Schaefer & Ringwald 1995). Schaefer (2010) adopts a median spectral type of the secondary from estimates culled from the literature of G5 IV.

The outburst mechanism for recurrent novae is thermonuclear runaway on the white dwarf triggered by the accreted mass exceeding a critical limit (Starrfield et al. 1985, 1988). The relatively short 10 year cycle of U Sco and the fast evolution of its outbursts imply that the white dwarf is close to the Chandrasekhar limit (e.g., Starrfield et al. 1988; Hachisu et al. 2000). Ejecta from previous outbursts were also found to be He-rich (Williams et al. 1981; Barlow et al. 1981; Anupama & Dewangan 2000; though this was contested by Iijima 2002), further fueling discussion of U Sco as a possible progenitor of a Type Ia supernova (e.g., Starrfield et al. 1988; Hachisu et al. 1999; Schaefer 2010; see, however, the evolutionary considerations of Sarna et al. 2006): Thoroughgood et al. (2001) characterized it as “the best Type Ia supernova progenitor currently known.”

The 2006 explosion of the recurrent nova RS Oph provided a cogent demonstration of the diagnostic power of prompt X-ray observations. RS Oph was a particularly bright X-ray source: the explosion occurs within the dense wind of the secondary red giant star, resulting in a $\sim 10^7$ – 10^8 K blast wave whose evolution was followed by *RXTE*, *Swift*, and *Chandra*

(Sokoloski et al. 2006; Bode et al. 2006; Nelson et al. 2008; Drake et al. 2009). Detailed three-dimensional hydrodynamic modeling of the blast by Orlando et al. (2009) provided estimates of the explosion energy, ejecta mass, and confirmed the presence of enhanced gas density in the equatorial plane of the system.

Spectroscopy of the 2010 outburst of U Sco found H_{α} and H_{β} H Balmer line profiles broadened by 7600 km s^{-1} full-width at half-maximum (Anupama 2010) and by $11,000 \text{ km s}^{-1}$ full-width at zero intensity (Arai et al. 2010), consistent with those observed in earlier outbursts (e.g., Barlow et al. 1981; Munari et al. 1999; Anupama & Dewangan 2000; Iijima 2002). If partially converted to thermal energy, analogous to the explosion of RS Oph into the dense wind of the secondary star, such kinetic energy would result in heating to X-ray emitting temperatures. While the secondary of U Sco lacks the cool, dense wind of the RS Oph secondary that provided the medium for copious X-ray production, the possibility of the blast generating significant X-rays from shocked ejecta or shocked gas in its accretion disk or ambient circumbinary material remained.

The early outburst was observed by the *Swift*, *RXTE*, and *International Gamma-Ray Astrophysics Laboratory (INTEGRAL)* satellites within a day of discovery (Schlegel et al. 2010; Manousakis et al. 2010) but all failed to detect any X-ray emission. Schlegel et al. (2010) placed the most stringent upper limit of $L_X < 1.1 \times 10^{-13} \text{ erg s}^{-1} \text{ cm}^{-2}$ (90% confidence) in the 0.3–10 keV band based on data obtained on 2010 January 29–30.

Here we describe detailed hydrodynamic simulations of the U Sco explosion similar to those undertaken for RS Oph by Orlando et al. (2009). We investigate the effects of the accretion disk and close secondary companion on the explosion, and examine possible constraints the lack of observed X-rays might provide.

Table 1
Adopted Parameters and Initial Conditions for the Hydrodynamic Models of the 2010 U Sco Explosion

| Parameter | Value | | | | | |
|---|---|--------------------|--------------------|--------------------|--------------------|--------------------|
| Secondary star radius | $R_b = 2.1 R_\odot$ | | | | | |
| Binary separation | $a = 6.5 R_\odot$ | | | | | |
| Inclination | $i = 83^\circ$ | | | | | |
| Model abbreviation | E44M-7 D13 | E44M-7 D15 | E43M-8 D15 | E44M-7 D15HW | E44M-7 D15LW | E45M-6 D15LW |
| Explosion energy, E_0 (erg) | 10^{44} | 10^{44} | 10^{43} | 10^{44} | 10^{44} | 10^{45} |
| Ejecta mass, M_{ej} (M_\odot) | 10^{-7} | 10^{-7} | 10^{-8} | 10^{-7} | 10^{-7} | 10^{-6} |
| Accn. disk density, n_d (cm^{-3}) | 10^{13} | 10^{15} | 10^{15} | 10^{15} | 10^{15} | 10^{15} |
| Sec. wind density, n_w (cm^{-3}) | 10^6 | 10^6 | 10^6 | 10^7 | 10^5 | 10^5 |
| Eq. enhancement, n_{eq} (cm^{-3}) | 10^8 | 10^8 | 10^8 | 10^9 | 10^7 | 10^7 |
| X-ray luminosity, L_X (erg s^{-1}) | 1×10^{33} | 5×10^{32} | 3×10^{31} | 4×10^{33} | 5×10^{31} | 7×10^{33} |
| <i>Swift</i> XRT, L_X (erg s^{-1}) | $< 2 \times 10^{33}$ (90% confidence) | | | | | |
| Spatial domain | $-6.6 \leq x \leq 6.6 \text{ AU}$ $0 \leq y \leq 6.6 \text{ AU}$ $0 \leq z \leq 6.6 \text{ AU}$ | | | | | |
| AMR max. resolution | $4 \times 10^8 \text{ cm}$ ($2.7 \times 10^{-5} \text{ AU}$) | | | | | |
| Time covered | 0–18 hr | | | | | |

2. HYDRODYNAMIC MODELING

The three-dimensional hydrodynamic model adopted here is similar to that of Orlando et al. (2009). The calculations were performed using FLASH, an adaptive mesh refinement multi-physics code for astrophysical plasmas (Fryxell et al. 2000). The hydrodynamic equations for compressible gas dynamics are solved using the FLASH implementation of the piecewise-parabolic method (PPM; Colella & Woodward 1984). Unlike the models of Orlando et al. (2009) computed for the case of RS Oph, for the very early phase of the blast studied here we do not take into account radiative losses and thermal conduction, assuming that the remnant is in its adiabatic expansion phase for the whole evolution considered. This assumption is valid if the time covered by our simulations t_{end} is smaller than the transition time from adiabatic to radiative phase for an expanding spherical blast, defined as (e.g., Blondin et al. 1998; Petruk 2005)

$$t_{\text{tr}} = 0.522 E^{4/17} n_{\text{med}}^{-9/17} \text{ s}, \quad (1)$$

where $E = E_0$ is the energy of the explosion and n_{med} is the particle number density of the ambient medium. As discussed below, it turns out that $t_{\text{end}} \ll t_{\text{tr}}$ in our set of simulations and our assumption is valid.

For the system parameters, we adopt the values of Thoroughgood et al. (2001); these are listed in Table 1, together with the parameters adopted for the blast models investigated here. We included a diffuse, puffed-up disk-like distribution around the system which is analogous to the gas density enhancement found in the numerical model of the RS Oph system immediately prior to outburst by Walder et al. (2008, see also Mastrodomos & Morris 1999) and to the equatorial gas distribution adopted by Orlando et al. (2009). We also included a flared, uniform density gas accretion disk around the white dwarf, adopting the shape from Hachisu et al. (2000). We included the secondary star as an impenetrable body. A close-up of this initial pre-blast configuration is illustrated in Figure 1.

As an initial condition, we assumed a spherical Sedov-type blast wave (Sedov 1959) originating from the thermonuclear explosion centered on the white dwarf, with radius $r_0 = 4 \times 10^5 \text{ km}$ and total energy E_0 . This energy was partitioned

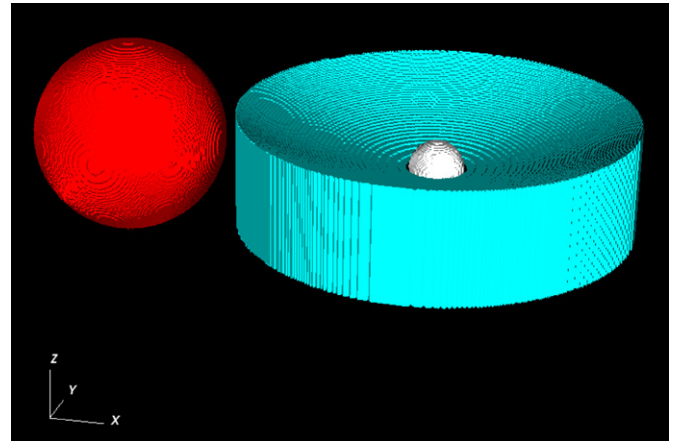


Figure 1. Rendition of the U Sco binary system model initial conditions. The white sphere represents the pre-outburst, initial radius of the Sedov-type blast on the white dwarf.

(A color version of this figure is available in the online journal.)

such that 1/4 was contained in thermal energy and 3/4 in kinetic energy. Solar abundances of Grevesse & Sauval (1998, GS) were assumed for the disk, wind, and equatorial ambient gas, while the ejecta metallicity was assumed to be enhanced by a factor of 10. This latter choice was guided by observations of He-rich ejecta in previous outbursts, as noted in Section 1, as well as the Drake et al. (2009) high-resolution X-ray spectroscopic study of the 2006 RS Oph blast that found evidence for metal-rich ejecta. Since radiative losses were not important for the early blast evolution, the choice of abundances is only relevant for computation of the emitted X-ray intensity of the blast.

Six models were computed to explore the effects of a different accretion disk and circumstellar gas density, explosion energy, and total ejecta mass on the outcome of the blast. Direct estimates of the ejecta mass from observations of the 1979 and 1999 outbursts (Williams et al. 1981; Anupama & Dewangan 2000; Evans et al. 2001) find $M_{ej} \sim 10^{-7} M_\odot$. Expansion velocities of $\sim 5000 \text{ km s}^{-1}$ from optical spectroscopy correspond to a kinetic energy of $2.5 \times 10^{43} \text{ erg}$, which can be taken as a lower limit to the explosion energy. This is consistent with

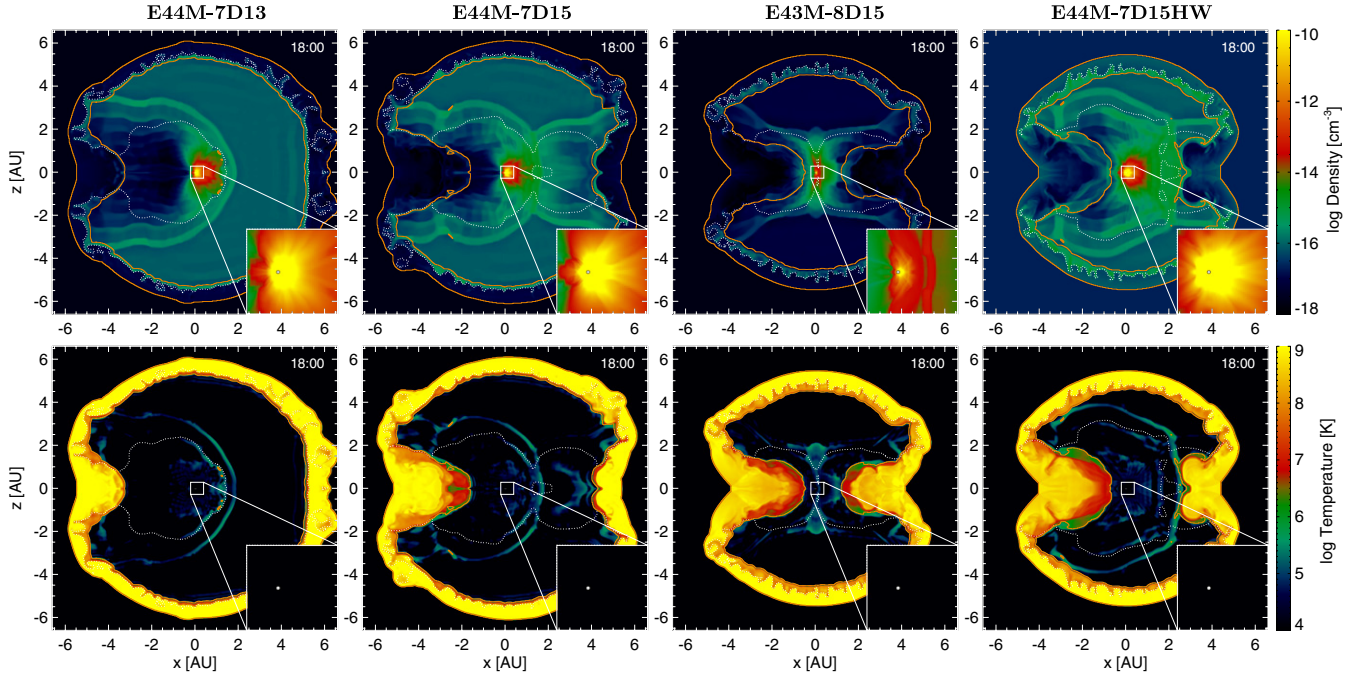


Figure 2. Color-coded cross-section images of the gas density distribution (top) and temperature (bottom) 18 hr after the U Sco blast, corresponding to the end of the hydrodynamic simulations. The secondary star is at the origin, and the white dwarf is to the right. The different panels illustrate models with accretion disk density $n_d = 10^{13} \text{ cm}^{-3}$ and an explosion energy of $E_0 = 10^{44} \text{ erg}$ (E44M-7D13; left); $n_d = 10^{15} \text{ cm}^{-3}$ and $E_0 = 10^{44} \text{ erg}$ (E44M-7D15; left-center); $n_d = 10^{15} \text{ cm}^{-3}$ and $E_0 = 10^{43} \text{ erg}$ (E43M-8D15; right-center). Far right panels show a similar model to the left-center panels, except with CSM gas densities increased by a factor of 10 (E44M-7D15HW). Inset panels show the blast structure closer to the system origin. The secondary star is shown and is responsible for the strong “shadowing” of the blast wave. The accretion disk is completely destroyed by the blast in all simulations. The white dotted contour encloses the ejecta. The red solid contour denotes the regions with plasma temperature $T > 1 \times 10^6 \text{ K}$.

(A color version of this figure is available in the online journal.)

estimates of the integrated optical output from earlier outbursts of 10^{44} erg (e.g., Webbink et al. 1987). We therefore adopted fiducial values of $E_0 = 10^{44} \text{ erg}$ and $M_{\text{ej}} = 10^{-7} M_{\odot}$ and explored the effects of lower and higher values of each by an order of magnitude. For the accretion disk, we assumed a uniform density of $n_d = 10^{15} \text{ cm}^{-3}$ and investigated a further model with $n_d = 10^{13} \text{ cm}^{-3}$. The wind and equatorial density enhancement are included for completeness. While this circumstellar gas is not expected to have a profound influence on the dynamics and evolution of the blast, it does influence the shock structure and the predicted X-ray luminosity. We probed the effects of increasing and decreasing the circumstellar gas density by a factor of 10.

The hydrodynamic equations were solved in one quadrant of the three-dimensional spatial domain and the coordinate system was oriented in such a way that both the white dwarf and the donor star lie on the x -axis. The donor star was at the origin of the coordinate system, $(x_0, y_0, z_0) = (0, 0, 0)$, and the white dwarf was located at $x = 0.03 \text{ AU}$, i.e., the system orbital separation. The extents of spatial domains employed for the different models are listed in Table 1 together with other relevant parameters and depended on the circumstellar gas density; two models that investigated lower densities for which expansion rates were greater required larger domains.

The explosion was followed for 18 hr in order to explore the early phase X-ray emission and capture the details of the effects of the explosion environment on the blast evolution. A major challenge in modeling the explosion of U Sco is the very small scale of the system compared with the size of the rapidly expanding blast wave. The separation of the two stars is only 0.03 AU —a distance traversed by a blast wave moving at

5000 km s^{-1} in less than 20 minutes—and the secondary star subtends a sufficiently large solid angle that it has a significant effect on the blast wave evolution. To capture this range of scales, the models explored here employed 16 nested levels of adaptive mesh refinement, with resolution increasing twice at each refinement level. This grid configuration yields an effective resolution of $\approx 4 \times 10^3 \text{ km}$ at the finest level, corresponding to ≈ 100 grid points per initial radius of the blast.

Given the parameters in Table 1, for five of our six models $t_{\text{tr}} > 3$ days from Equation (1), and for the sixth (E44M-7D15HW) $t_{\text{tr}} = 2.3$ days. These times are much larger than the time covered by our simulations. Our modeled remnants therefore never enter the radiative phase.

3. RESULTS AND DISCUSSION

3.1. Temperature and Density Structure

The U Sco models all evolved quite differently to those presented for RS Oph by Orlando et al. (2009). As noted in Section 1, this difference is expected because U Sco lacks the dense wind of RS Oph for propagation of an X-ray emitting blast wave.

The 18 hr post-blast gas density and temperature distributions in the $x-z$ plane bisecting the system (the plane of the orbital axis; the accretion disk is edge on) are illustrated in Figure 2. All the models exhibit conspicuous departure from spherical symmetry. The main feature of the gas density distribution is a large cavity to the left of the figures (negative x -direction), which is a blast wave “shadow” cast by the secondary star. This result reinforces the need to perform simulations with sufficient

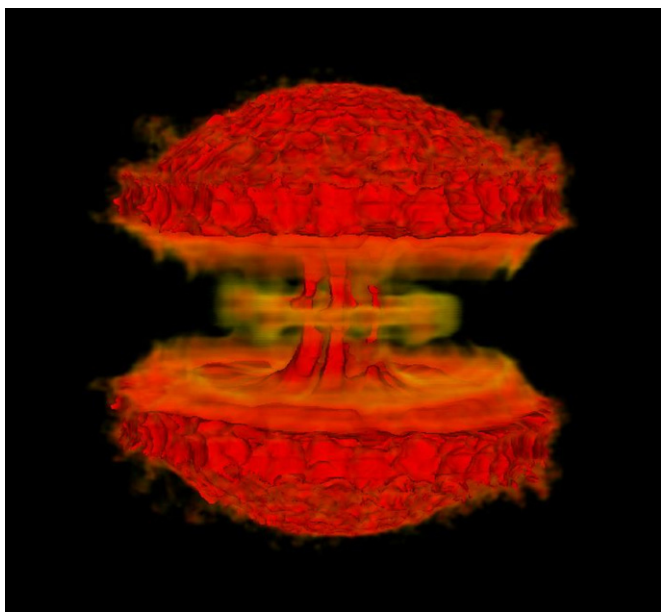


Figure 3. Three-dimensional rendering of the ejecta distribution, 18 hr after the blast for the model E44M-7D15. The plane of the orbit of the central binary system lies on the (x, y) plane.

(A color version of this figure is available in the online journal.)

spatial resolution to capture the details of the pre-blast system configuration.

In all models, the accretion disk is completely destroyed by the blast. This is not surprising considering the gravitational binding energy of the disk in our models is 3–4 orders of magnitude lower than the explosion energy: disk destruction is assured unless the disk gas density is substantially higher than 10^{15} cm^{-3} . Wouters et al. (2010; see also Munari et al. 2010) report a renewed optical flickering with amplitude “0.2 mag over the course of an hour” on 2010 February 5. They interpret this re-establishment of accretion, implying a limit of 7 days on the build-up of an angular momentum shedding accretion disk. In our simulations, the disk volume is $V_{\text{disk}} \approx 2 \times 10^{34} \text{ cm}^3$ and its mass ranges between $2.2 \times 10^{-10} M_{\odot}$ (model E44M-7D13) and $2.2 \times 10^{-8} M_{\odot}$ (all other models). The build-up of the disk in 7 days would imply a rate of mass loss from the companion star ranging between 10^{-8} and $10^{-6} M_{\odot} \text{ yr}^{-1}$, consistent with the estimate of Hachisu et al. (2000). We note, however, that any renewed disk build-up would need to overcome the dynamic pressure of the radiatively driven outflow from the evolving central object.

Model E44M-7D13, with lower accretion disk gas density, shows only a very small effect of the disk in a slight inhibition of the blast wave progress in the positive x -direction. In contrast, the higher disk gas density in all the other models has quite a profound effect on the blast evolution. Both the blast and ejecta are strongly collimated in polar directions, the collimation being more prominent for lower explosion energy (E43M-8D15) as might be expected. Figure 3 shows, as an example, the collimation of ejecta 18 hr after the outburst for the model E44M-7D15. Kato & Hachisu (2003) interpreted “horned” optical line profiles observed in previous U Sco outburst (e.g., Munari et al. 1999) as evidence for “jet-shaped” outflows. Similar blast collimation was both predicted by hydrodynamic simulations of the early RS Oph blast by Walder et al. (2008) and Orlando et al. (2009), and deduced through X-ray spectroscopy obtained 13.6 days after the outburst (Drake et al. 2009).

The simulations indicated the collimation was caused by an equatorial disk-like gas distribution around the white dwarf. High spatial resolution observations of the blast at various times also found optical, infrared, radio, and X-ray collimation signatures (O’Brien et al. 2006; Bode et al. 2007; Chesneau et al. 2007; Luna et al. 2009).

Evidence for a more strongly collimated synchrotron radio jet was also found by Rupen et al. (2008) and Sokoloski et al. (2008). The latter authors concluded that such structure is too highly collimated to be explained by the influence of circumbinary material on the explosion. The calculations presented here and by Orlando et al. (2009) bring such conclusions into question: the nature of the explosion environment is crucial for the morphology of the evolving blast and ejecta. While the models presented here do not produce obvious narrow jets of material, we note that radio synchrotron emission also depends strongly on the magnetic field strength, gradient, and orientation (e.g., Orlando et al. 2007) and need not be co-spatial with obvious density enhancements in the ejecta.

The outer regions of the blast are characterized by a layer of shocked circumstellar medium (CSM) with temperature $\approx 10^9 \text{ K}$ and a thin expanding surface of shocked ejecta with temperature in the range $(10^7\text{--}10^8) \text{ K}$ (see Figure 2). The CSM gives rise to a reflected shock that heats the ejecta and is strongest for model E44M-7D15HW in which the CSM density is highest. The secondary star also gives rise to a prominent “bow shock,” though in this structure the gas is shocked to a temperature of only a few 10^5 K and does not give rise to any conspicuous observable X-ray emission. It is worth noting that Figure 2 reports the proton temperature set by collisionless heating at the shock front. Given the short timescale considered here, protons and electrons are likely not thermalized at the forward shock, so that the ratio of the electron to proton temperature at the blast wave is expected to be $(T_e/T_p) < 1$. Ghavamian et al. (2007) derived a physical model for the heating of electrons and protons in strong shocks that predicts a relationship $(T_e/T_p) \propto v_s^{-2}$, where v_s is the shock velocity. Considering the velocity of the forward shock in our simulations is of the order of $10,000 \text{ km s}^{-1}$, from Figure 2 of Ghavamian et al. (2007) we derive $(T_e/T_p) < 0.1$. Thus, we expect that the electron temperature of the shocked CSM is $\approx 10^8 \text{ K}$. X-rays are instead naturally dominated by the higher density parts of the shocked ejecta which are expected to equilibrate quickly. In the following, we therefore assumed electron–proton temperature equilibration in shocked ejecta.

3.2. X-ray Luminosity and Morphology

X-ray emission from the blast was synthesized from the model results using the methodology described by Orlando et al. (2009). The synthesis includes thermal broadening of emission lines, the Doppler shift of lines due to the component of plasma velocity along the line of sight, and photoelectric absorption by the interstellar medium (ISM), CSM, and ejecta. The absorption by the ISM is calculated assuming a column density $N_H = 1.4 \times 10^{21} \text{ cm}^{-2}$ (e.g., Kahabka et al. 1999, and is consistent with a distance to U Sco of 12 kpc, e.g., Schaefer 2010); the local absorption is calculated as due to shocked CSM (assuming GS abundances) and ejecta (GS abundances $\times 10$). The X-ray emission from the blast at 18 hr is illustrated for four representative models in Figure 4. The absorption by the ejecta contributes to a small difference between the predicted X-ray luminosities of the different models. Most of the emission arises from the high-temperature shocked ejecta

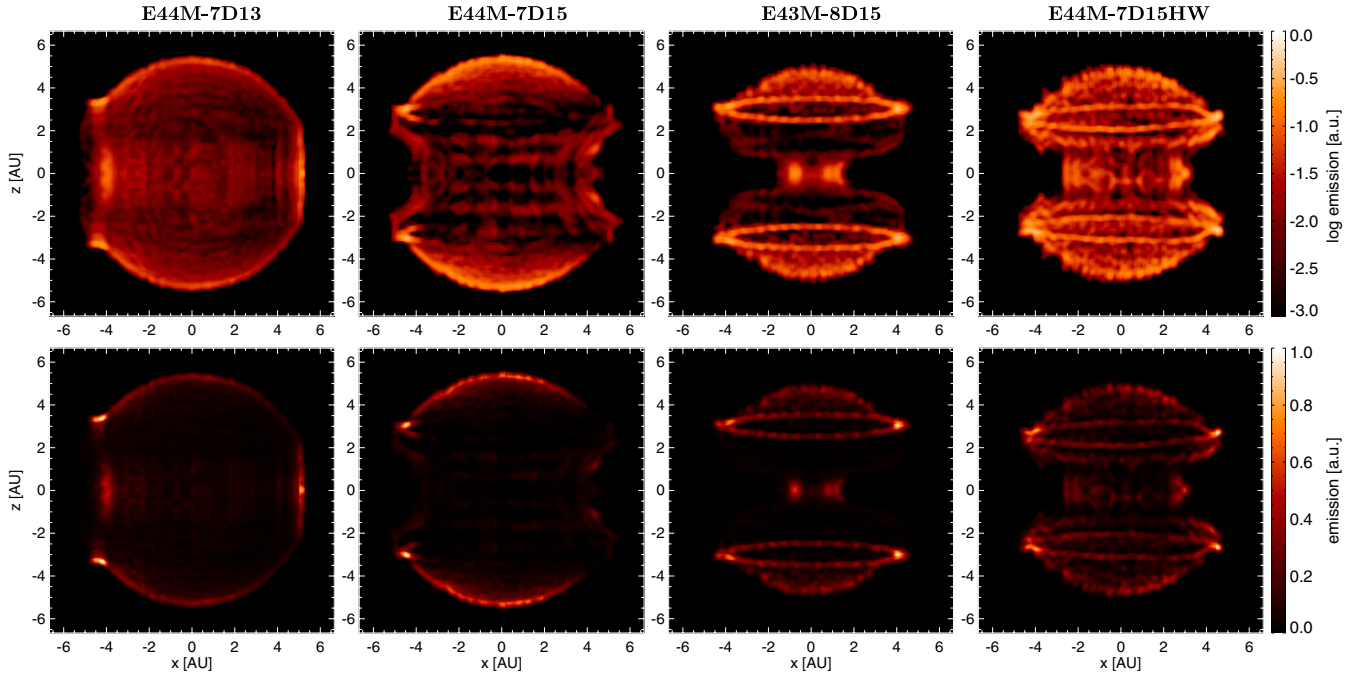


Figure 4. X-ray images (normalized to the maximum of each panel) projected along the line of sight of the blast after 18 hr of evolution, corresponding to the density and temperature distributions illustrated in Figure 2. Upper panels are rendered with a logarithmic surface brightness scale and lower panels with a linear scale. The plane of the orbit is inclined by 7° to the line of sight. Both the secondary subgiant and the white dwarf lie on the x -axis. Most of the X-ray emission originates from shocked ejecta.

(A color version of this figure is available in the online journal.)

forming the outer “shell” of the blast wave where we assumed electron–proton temperature equilibration. Model E44M-7D13 exhibits significant equatorial brightening that arises from a ring of higher density ejecta that was partially impeded by the accretion disk. This structure is not present in models E44M-7D15, E43M-8D15, and E44M-7D15HW, with a higher density disk. Instead, these latter models are dominated by bipolar cusps that appear either limb-brightened (E44M-7D15), or forming ring-like structures (E43M-8D15 and E44M-7D15HW), in the projected image, accompanied by limited equatorial emission.

The X-ray luminosities of the simulations in the (0.6–12.4) keV band are listed in Table 1 and vary between $L_X = 3 \times 10^{31}$ erg s $^{-1}$ (E43M-7D15) and 7×10^{33} erg s $^{-1}$ (E45M-6D15LW). The X-ray luminosity is larger for higher ejecta mass, explosion energy, and circumstellar gas density. The X-ray flux upper limit of $F_X < 1.1 \times 10^{-13}$ erg s $^{-1}$ cm $^{-2}$ obtained at a similar epoch to our simulations by Schlegel et al. (2010) corresponds to an X-ray luminosity of $L_X = 2 \times 10^{33}$ erg s $^{-1}$ for a distance of 12 kpc. The fact that the models with $M_{ej} = 10^{-7} M_\odot$ predict X-ray luminosities close to the *Swift* upper limit (except run E44M-7D15LW whose luminosity is much lower), while the model with $M_{ej} = 10^{-6} M_\odot$ and lower circumstellar density (E45M-6D15LW) exceeds it, suggests that the mass of ejecta in the 2010 outburst was not significantly larger than $10^{-7} M_\odot$. This is consistent with estimates of previous outbursts in 1979 and 1999 (Williams et al. 1981; Anupama & Dewangan 2000; Evans et al. 2001). While we cannot rule out with certainty the circumstellar density being even lower than assumed in the latter model with $M_{ej} = 10^{-6} M_\odot$, which could reduce the predicted X-ray luminosity and reconcile it with the *Swift* upper limit, such a large mass requires the larger assumed explosion energy of 10^{45} erg to take the ejecta out of the gravitational well of the system. This exceeds by an order of

magnitude the total explosion energy of 10^{44} erg estimated for previous outbursts by Webbink et al. (1987).

The model with a higher wind and equatorial gas density (E44M-7D15HW) has a stronger X-ray contribution from ejecta heated in the reflected shock that *exceeds* the observed X-ray upper limit. This is consistent with our assumption of a rather low circumstellar gas density, commensurate with the evolutionary state of the U Sco component stars, and does not alter the conclusion that the ejected mass was probably not larger than $10^{-7} M_\odot$.

J.J.D. was funded by NASA contract NAS8-39073 to the Chandra X-ray Center. FLASH was developed by the DOE-supported ASC/Alliance Center for Astrophysical Thermonuclear Flashes, University of Chicago. Simulations were executed at the HPC SCAN facility of INAF-OAPA.

REFERENCES

- Anupama, G. C. 2010, ATel, **2411**, 1
 Anupama, G. C., & Dewangan, G. C. 2000, *AJ*, **119**, 1359
 Arai, A., Yamanaka, M., Sasada, M., & Itoh, R. 2010, CBET, **2152**, 1
 Barlow, M. J., et al. 1981, MNRAS, **195**, 61
 Blondin, J. M., Wright, E. B., Borkowski, K. J., & Reynolds, S. P. 1998, *AJ*, **500**, 342
 Bode, M. F., Harman, D. J., O’Brien, T. J., Bond, H. E., Starrfield, S., Darnley, M. J., Evans, A., & Eyres, S. P. S. 2007, *AJ*, **665**, L63
 Bode, M. F., et al. 2006, *AJ*, **652**, 629
 Chesneau, O., et al. 2007, *A&A*, **464**, 119
 Colella, P., & Woodward, P. R. 1984, *J. Comput. Phys.*, **54**, 174
 Drake, J. J., et al. 2009, *AJ*, **691**, 418
 Evans, A., Krautter, J., Vanz, L., & Starrfield, S. 2001, *A&A*, **378**, 132
 Fryxell, B., et al. 2000, *ApJS*, **131**, 273
 Ghavamian, P., Laming, J. M., & Rakowski, C. E. 2007, *AJ*, **654**, L69
 Grevesse, N., & Sauval, A. J. 1998, *Space Sci. Rev.*, **85**, 161
 Hachisu, I., Kato, M., Kato, T., Matsumoto, K., & Nomoto, K. 2000, *AJ*, **534**, L189

- Hachisu, I., Kato, M., Nomoto, K., & Umeda, H. 1999, *ApJ*, **519**, 314
- Iijima, T. 2002, *A&A*, **387**, 1013
- Johnston, H. M., & Kulkarni, S. R. 1992, *ApJ*, **396**, 267
- Kahabka, P., Hartmann, H. W., Parmar, A. N., & Negueruela, I. 1999, *A&A*, **347**, L43
- Kato, M., & Hachisu, I. 2003, *ApJ*, **587**, L39
- Luna, G. J. M., Montez, R., Sokoloski, J. L., Mukai, K., & Kastner, J. H. 2009, *ApJ*, **707**, 1168
- Manousakis, A., Revnivtsev, M., Krivonos, R., & Bozzo, E. 2010, *ATel*, **2412**, 1
- Mastrodemos, N., & Morris, M. 1999, *ApJ*, **523**, 357
- Munari, U., Dallaporta, S., & Castellani, F. 2010, *IBVS*, **5930**, 1
- Munari, U., et al. 1999, *A&A*, **347**, L39
- Nelson, T., Orio, M., Cassinelli, J. P., Still, M., Leibowitz, E., & Mucciarelli, P. 2008, *ApJ*, **673**, 1067
- O'Brien, T. J., et al. 2006, *Nature*, **442**, 279
- Orlando, S., Bocchino, F., Reale, F., Peres, G., & Petruk, O. 2007, *A&A*, **470**, 927
- Orlando, S., Drake, J. J., & Laming, J. M. 2009, *A&A*, **493**, 1049
- Petruk, O. 2005, *J. Phys. Stud.*, **9**, 364 (http://www.ktf.franko.lviv.ua/JPS/2005/4/abs/a364_373.html)
- Rupen, M. P., Mioduszewski, A. J., & Sokoloski, J. L. 2008, *ApJ*, **688**, 559
- Sarna, M. J., Ergma, E., & Gerskevits, J. 2006, *Acta Astron.*, **56**, 65
- Schaefer, B. E. 1990, *ApJ*, **355**, L39
- Schaefer, B. E. 2010, *ApJS*, **187**, 275
- Schaefer, B. E., Harris, B. G., Dvorak, S., Templeton, M., & Linnolt, M. 2010, *IAU Circ.*, **9111**, 1
- Schaefer, B. E., & Ringwald, F. A. 1995, *ApJ*, **447**, L45
- Schlegel, E. M., et al. 2010, *ATel*, **2419**, 1
- Sedov, L. I. 1959, *Similarity and Dimensional Methods in Mechanics* (New York: Academic Press)
- Sokoloski, J. L., Luna, G. J. M., Mukai, K., & Kenyon, S. J. 2006, *Nature*, **442**, 276
- Sokoloski, J. L., Rupen, M. P., & Mioduszewski, A. J. 2008, *ApJ*, **685**, L137
- Starrfield, S., Sparks, W. M., & Shaviv, G. 1988, *ApJ*, **325**, L35
- Starrfield, S., Sparks, W. M., & Truran, J. W. 1985, *ApJ*, **291**, 136
- Thoroughgood, T. D., Dhillon, V. S., Littlefair, S. P., Marsh, T. R., & Smith, D. A. 2001, *MNRAS*, **327**, 1323
- Walder, R., Folini, D., & Shore, S. N. 2008, *A&A*, **484**, L9
- Webbink, R. F., Livio, M., Truran, J. W., & Orio, M. 1987, *ApJ*, **314**, 653
- Williams, R. E., Sparks, W. M., Gallagher, J. S., Ney, E. P., Starrfield, S. G., & Truran, J. W. 1981, *ApJ*, **251**, 221
- Worters, H. L., Eyres, S. P. S., Rushton, M. T., & Schaefer, B. 2010, *IAU Circ.*, **9114**, 1